Eur. Phys. J. B **40**, 433–437 (2004)
DOI: 10.1140/epjb/e2004-00228-4

THE EUROPEAN PHYSICAL JOURNAL B

Emission wavelength engineering of InAs/InP(001) quantum wires

D. Fuster[1], L. González[1,a], Y. González[1], J. Martínez-Pastor[2], T. Ben[3], A. Ponce[3], and S.I. Molina[3]

[1] Instituto de Microelectrónica de Madrid (CNM-CSIC), Isaac Newton 8, 28760 Tres Cantos, Madrid, Spain
[2] Instituto de Ciencia de los Materiales, Universidad de Valencia, P.O. Box 2085, 46071 Valencia, Spain
[3] Departamento de Ciencia de los Materiales e I. M. y Q. I., Universidad de Cádiz, Puerto Real, Cádiz, Spain

Received 16 December 2003
Published online 3 August 2004 – © EDP Sciences, Società Italiana di Fisica, Springer-Verlag 2004

Abstract. In this work we have studied the dependence of the optical properties of self-assembled InAs quantum wires (QWr) grown on InP(001) on the growth temperature of the InP cap layer, as a mean for controlling the InAs QWr size. Our main result is that we can tune the emission wavelength of InAs QWr either at 1.3 μm or 1.55 μm at room temperature. We suggest that the role of growth temperature is to modify the As/P exchange at the InAs QWr/InP cap layer interface and consequently the amount of InAs involved in the nanostructure. In this way, due to the enhancement of the As/P exchange, the higher the growth temperature of the cap layer, the smaller in height the InAs quantum wires. Accordingly, the emission wavelength is blue shifted with InP cap layer growth temperature as the electron and hole ground state moves towards higher energies. Optical studies related to the dynamics of carrier recombination and light emission quenching with temperature are also included.

PACS. 81.16.Dn Self-assembly – 78.67.Lt Quantum wires – 81.07.Vb Quantum wires

1 Introduction

It is well known that the use of semiconductor nanostructures as active region of lasers can give rise to devices with a low threshold current and other advantageous properties. For their use in telecommunications, this type of lasers should emit at wavelengths $\lambda = 1.30$ μm and 1.55 μm. Recent works [1] have pointed out that self-assembled quantum wires (QWr) obtained by molecular beam epitaxy (MBE) growth of InAs on InP(001) could be good candidates for the active region of emitters in these wavelengths.

Given that the optical properties of nanostructures for a certain heteroepitaxial system basically depend on their size, we should be able to control this parameter in order to design their emission wavelength. In this paper we propose a method for controlling the QWr size in order to tune the emission wavelength of the InAs QWr. This is based on the variation of the growth temperature of the InP cap layer, because this parameter controls the extent of the As/P exchange [2] and consequently could be responsible of the amount of InAs involved in the nanostructure. Our experimental results show that we can obtain room temperature (RT) photoluminescence (PL) in this system at 1.3 μm or 1.55 μm. We also investigate some aspects of the exciton recombination dynamics.

[a] e-mail: `luisa@imm.cnm.csic.es`

2 Experimental

The samples under study consist of a 100 nm thick InP buffer layer grown by MBE on InP(001) substrate followed by a 1.6 monolayer (ML) thick InAs layer deposited at a substrate temperature $T_s = 515$ °C, beam equivalent pressure $\mathrm{BEP(As_4)} = 2.3 \times 10^{-6}$ mbar, and a growth rate of 0.1 ML/s in a pulsed dynamic way (pulsed indium cell sequence: 1s ON/2s OFF). The deposited InAs thickness corresponds to the critical thickness to form the QWr, when the $[1\bar{1}0]$ reflection high-energy electron diffraction (RHEED) pattern shows the 2D-3D transition [1,3]. Finally, a 20 nm thick cap layer is grown at a substrate temperature $T_s = 515$ °C, by MBE (High T sample), and $T_s = 380$ °C, by atomic layer molecular beam epitaxy (ALMBE) [4] (Low T sample). For the ALMBE grown InP cap layer, the stoichiometry of the growth front is controlled by means of the reflectivity difference (RD) technique in order to obtain InP planar surfaces [5]. A similar sample has been grown without cap layer for atomic force microscopy (AFM) measurements.

Contact mode AFM characterization has been performed *ex situ* in a home made AFM using commercial tips. The PL of the samples was excited by the 514.5 nm $\mathrm{Ar^+}$ laser line, dispersed by a 0.22 m focal length monochromator and synchronously detected with a cooled Ge photodiode. For polarized light emission measurements, the [110] direction of the samples is oriented at 45°

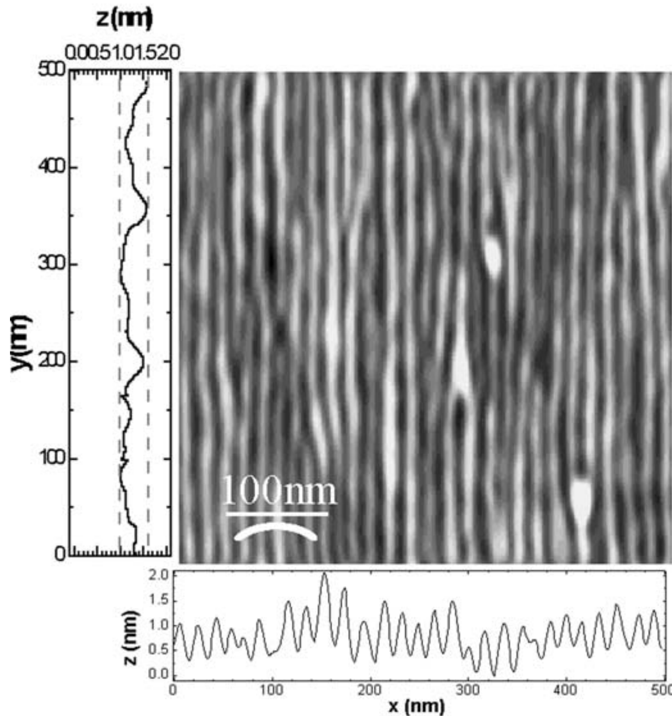

Fig. 1. 0.5×0.5 μm^2 atomic force microscopy (AFM) image of InAs quantum wires along [1$\overline{1}$0], grown on InP(001). Profiles along wire direction [1$\overline{1}$0], and [110] direction (crossing the wires) are shown on the left and bottom of the image.

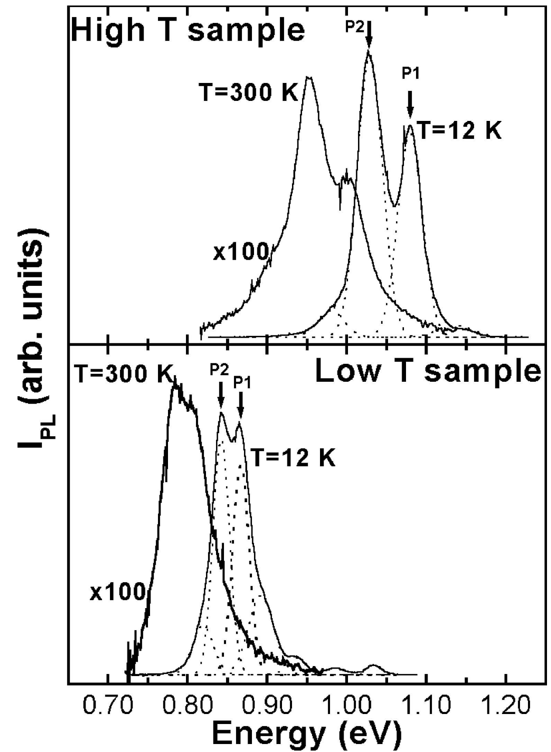

Fig. 2. Photoluminescence spectra of InAs quantum wires covered by 20 nm thick InP cap layer grown at substrate temperature T_s = 515 °C and T_S = 380 °C, named High T and Low T samples, respectively. The several Gaussians resolved are shown by dotted lines.

with respect to the polarization direction of the laser to get balanced pumping along both ⟨110⟩ directions and avoid polarization effects from the grating grooves. A Glann-Thomson polarizer at the entrance of the monochromator is used to measure the PL intensity along both principal directions.

For time resolved photoluminescence (TRPL) experiments, the sample was excited at 730 nm by a green-Nd:YAG (Verdi, Coherent) pumped mode-locked Ti:sapphire (Mira 900D, Coherent) laser, providing 2 ps pulses at a repetition rate of 76 MHz. The PL signal was dispersed by a single 0.5 m focal length imaging spectrometer and detected by a synchroscan streak camera (Hamamatsu C5680) with a type S1 cooled photocathode. The overall time response of the system in the widest temporal window (2 ns) was around 40–50 ps (full width at half maximum).

Cross section transmission electron microscopy (XTEM) characterization have been carried out in a JEOL 1200EX (120 kV) and 3000F (200 kV). The samples were prepared by mechanical thinning and ion milling at N_2 liquid temperature to minimize damages.

3 Results and discussion

Figure 1 shows an AFM image of the InAs QWr in the sample without InP cap layer. A histogram of the wire heights measured from several AFM profiles along [110] direction is well represented by a Gaussian distribution centered at 2 nm and having a linewidth of 0.9 nm. The wires are oriented along the direction [1$\overline{1}$0] and periodically arranged along the [110] direction with a period of 18 nm. They have an average length around 1 μm and a typical height fluctuation of 0.6 nm (∼2 ML, considering 1 InAs ML = 0.3 nm) within a single wire.

The PL spectra of the High T and Low T samples measured at low and room temperature (RT) are reported in Figure 2. The main emission peak at room temperature is located around 0.95 eV (1.3 μm) and 0.8 eV (1.55 μm) for high and low T samples, respectively. Their PL spectra can be well reproduced by the sum of several Gaussian emission components, which are represented by dotted lines in Figure 2. The energy distance between two adjacent emission peaks in the multi-line photoluminescence spectrum corresponds to 1 ML height fluctuation [6,7]. In a previous work [7] we proposed a model to obtain the single electron and hole states of an infinite array of rectangular biaxial strained QWr. According to this model and the previous assumption (1 ML height fluctuation between adjacent peaks), we obtain that the most intense Gaussian components shown in Figure 2, P1 and P2 would correspond to absolute wire heights of 10 and 11 ML for the Low T sample and 5 and 6 ML for the High T sample. This means a wire height increase of around 5 ML by decreasing the InP cap layer growth temperature from 515 °C to 380 °C. In fact, this is what we obtain by XTEM

Table 1. Average values of height and width of the buried QWr, contained in the samples for optical characterization, measured by cross section transmission electron microscopy (TEM).

Sample	Height (nm)	Width (nm)
High T	1.4 ± 0.3	10 ± 2
Low T	2.5 ± 0.5	10 ± 2

characterization of these samples. The geometric values of the buried InAs QWr for both samples measured by XTEM are listed in Table 1. The height corresponding to High T and Low T samples are about 5 ML and 8 ML respectively. These values agree with those predicted in our previous work, where we also pointed out that the estimate was affected by a reasonable error of 1-2 ML [7]. At the same time, it is also worth noting the fact that the wire height does not change appreciably after the InP capping process at low temperature, when comparing the XTEM value with that obtained from AFM characterization.

As the InAs QWr were grown under identical conditions (substrate temperature and arsenic pressure), the only difference between these samples is the substrate temperature, T_s, used to grow the InP cap layer. This means that the role of T_s for the growth of the InP cap layer is to change the QWr size. A possible explanation for the observed change on QWr size is the As/P exchange mechanism at the InAs/InP interface, which clearly should depend on temperature [2]. In this way, the higher the growth temperature of the cap layer, the smaller the height of the obtained InAs QWr due to an enhancement of the As/P exchange. Experiments based on *in situ* accumulated stress measurements to assess the role of the As/P exchange in QWr size reduction are presently under way.

PL results under polarized detection conditions at low temperature are shown in Figure 3. The maximum PL signal was obtained when the detection polarization was parallel to the direction [$1\bar{1}0$], i.e., along the wire axis, as marked in Figure 1. The PL polarization degree, defined as $P = (I_\parallel - I_\perp)/(I_\parallel + I_\perp)$, where $I_\parallel$ and $I_\perp$ are the PL signals detected under polarized light parallel and perpendicular to the self-assembled QWr, respectively, is also shown in Figure 4. The observed strong anisotropy reflected by P is a typical signature of the QWr emission [1,8] and its value does not depend on temperature. On the other hand, the polarization degree measured for the High T sample (∼15%) is lower than the corresponding one in the Low T sample (∼20%). This difference can be related to the shallower (less confined) nature of the electron and hole states in the first case and hence a higher degree of wave function penetration into the barriers. This result is consistent with the smaller size of the wires found in the High T sample [8].

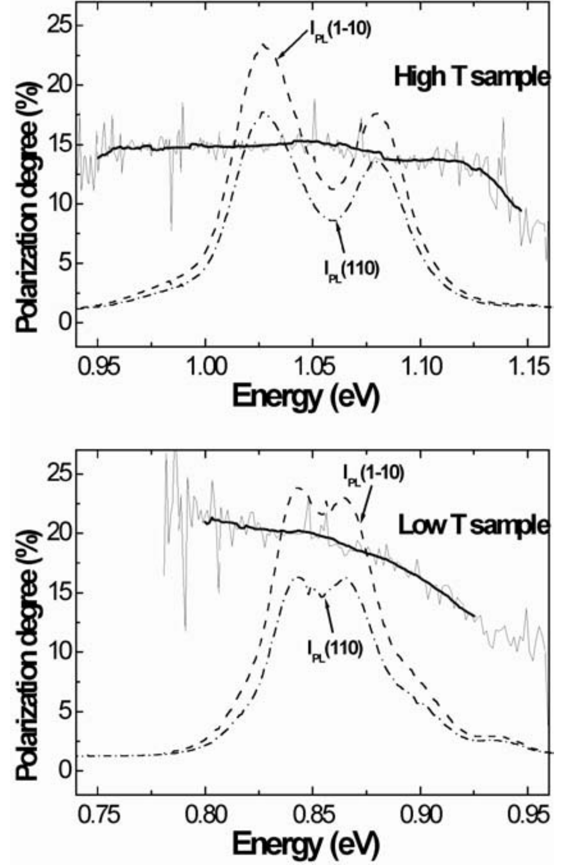

Fig. 3. Polarized photoluminescence spectra measured at 12 K of the High T and Low T samples of InAs quantum wires along [$1\bar{1}0$] (dashed lines) and [110] (dash-pointed lines). The polarization degree (experimental and smoothed continuous line) is indicated in vertical axis.

For using these structures in optoelectronic devices, it is also necessary to investigate the non-radiative mechanisms limiting their operation at RT. The evolution of the overall PL integrated intensity with T is shown in Figure 4. In both kind of samples the overall PL integrated intensity at room temperature is two orders of magnitude lower than that measured at 12 K. Therefore, their optical emission efficiency should not be too much different, even if the carrier confinement is expected to be appreciably different given the different QWr height in High T and Low T samples,

The experimental temperature dependence of the PL integrated intensity shown in Figure 4 clearly exhibit two different slopes in low (<100 K) and high (>100 K) temperature regions. It can be accounted for by a Boltzmann model for excitonic recombination with two quenching mechanisms [9]:

$$I_{\mathrm{PL}}(T) = \frac{I_0}{1 + \tau_0[\Gamma_1 \mathrm{e}^{-E_1/kT} + \Gamma_2 \mathrm{e}^{-E_2/kT}]} \quad (1)$$

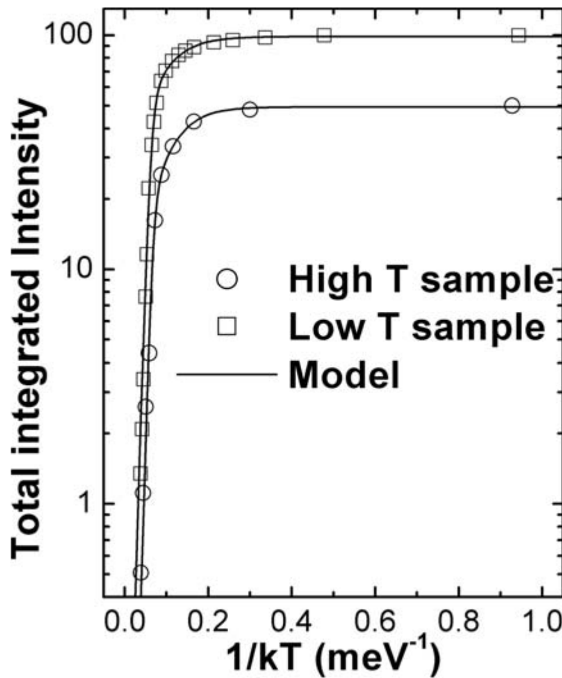

Fig. 4. Arrhenius plot of the PL integrated intensity for the High T and the Low T samples and best fitting curves according to a Boltzmann model for excitonic recombination.

where I_0 is the integrated PL intensity at 0 K, E_1 and E_2 are the activation energies of the two quenching mechanisms, Γ_1 and Γ_2 the two related scattering rates, τ_0 the radiative recombination time of excitons in QWr, assumed to be constant and fixed to 1 ns [10] and k is the Boltzmann constant. The best fitting parameters of the whole PL band quenching to equation (1) are shown in Table 2, which are similar to those obtained in reference [7] for previous studied samples grown under similar conditions to that used for the Low T sample. The low activation energy (E_1) determines the low temperature quenching of the PL and could be associated to carrier recombination through impurities in the nanostructure or its interfaces with the InP surrounding material [7]. The higher activation energy (E_2) is associated with the high temperature quenching of the PL band, and hence is the parameter to be associated to the intrinsic non-radiative recombination mechanism in self-assembled QWr. It is already well established that the most important temperature dependent non-radiative mechanism in quantum wells is the thermal escape of carriers towards the barrier material, either ambipolar [9] or unipolar [11]. This mechanism can be also appropriate in the case of QWr. If the PL quenching mechanism was the ambipolar thermal escape of correlated electron – hole pairs towards the InP barriers, we would expect an average escape energy (difference between the PL central energy and the InP bandgap energy) about 360 and 550 meV for High and Low T samples, respectively. These values are well above the values obtained for E_2 in the fit of experimental results in both samples to equation (1) (see Tab. 2). On the other hand, the expected energies for unipolar thermal escape of electrons (holes) are about 100 (290) and 180 (370) meV for the central PL energy in High T and Low T samples, respectively, as given by our previous calculations in reference [7]. Despite the differences between these values and those given in Table 2 (affected with an absolute error of 20–30 meV), the unipolar thermal escape of electrons towards the InP barriers could be the most probable non-radiative quenching mechanism limiting the emission of our samples at RT. More insight into this question can be obtained with a more detailed study based on the comparison between continuous wave and time resolved PL experiments as a function of temperature, as it is being carried out at present. Let us give here some previous results, which shows that the recombination dynamics is not very simple.

Figure 5 shows the PL transients measured at 12 and 230 K for a detection energy corresponding to the P2 peak of the High T sample. In the Low T sample the PL transients cannot be measured at a comparable incident power because the response of the streak camera photocathode

Table 2. Best fitting parameters to the experimental temperature dependence of the PL integrated intensity by using equation (1) for High T and Low T samples.

Sample	Γ_1 (s^{-1})	Γ_2 (s^{-1})	E_1(meV)	E_2(meV)
High T	2.7×10^9	8×10^{12}	20	140
Low T	3.5×10^9	20×10^{12}	21	145

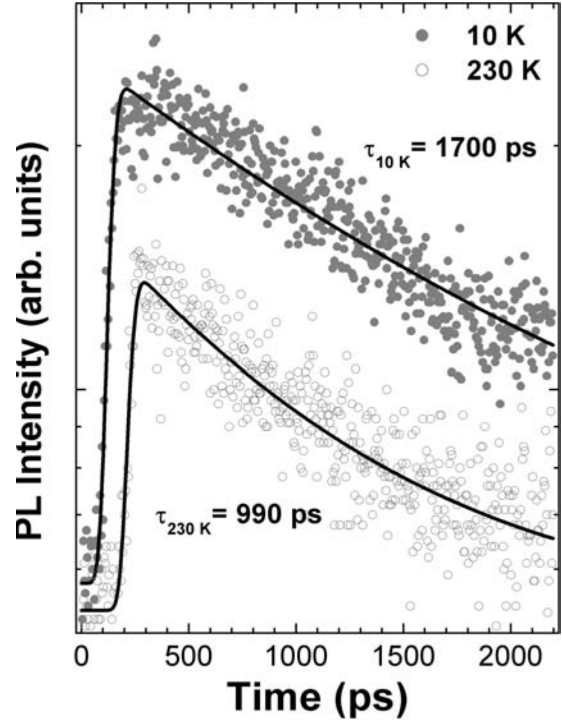

Fig. 5. Photoluminiscence transients of the High T sample P2 peak measured at 10 K (full dots) and 230 K (empty dots). We have represented in continuous line the mono-exponential decay convoluted with the system response fit. The decay times obtained from the best fits are included in the figure.

fastly decreases above 1200 nm. The experimental PL transients measured at low excitation densities can be nicely fitted to a mono-exponential decay, as shown in Figure 5 (continuous lines). We find 1700 and 990 ps for 12 and 230 K, respectively, and intermediate values between these temperatures. The large value found at the lowest temperature can be taken as mostly representative of the radiative recombination of the photogenerated excitons. At the same time, non-radiative recombination of excitons is taking place over the whole temperature range because the PL decay time is decreasing from 12 to 230 K. However, the time decay decreases less than a factor two between 12 and 230 K, where the continuous wave PL decreases more than one order of magnitude. This indicates that exciton localization effects can be present in our QWr, possibly related to height fluctuations along the wire direction, as observed in the AFM profiles (see Fig. 1). Although these results have been obtained in the High T sample, they can be extended to the Low T sample since the temperature evolution of the integrated PL intensity is similar in both samples and we do not expect any influence of the capping process in the exciton recombination dynamics.

4 Conclusions

We have developed a process for controlling the height of InAs QWr nanostructures grown on InP (001) substrate, and consequently their optical emission wavelength. It is based on the control of the growth temperature of the InP cap layer and probably relies on the dependence with temperature of the As/P exchange process at the InAs/InP interface that controls the amount of InAs involved in the nanostructures. In this way, the average height of the InAs QWr can be reduced up to 6 ML by changing the growth temperature from 380 °C to 515 °C and this fact allows us to obtain emission wavelengths at 1.3 and 1.55 μm at RT. We also can conclude that the quenching mechanism limiting the emission of these samples at RT is due to unipolar thermal escape of electrons towards the InP barriers, even if exciton localization effects can be present in our QWr.

This work was partially supported by Spanish MCyT under project No. TIC2002-04096-C03 and by Nanomat project of the EC Growth program, contract n° G5RD-CT-2001-00545. D. Fuster thanks the Spanish MCyT for funding.

References

1. L. González, J.M. García, R. García, F. Briones, J. Martínez-Pastor, C. Ballesteros, Appl. Phys. Lett. **76**, 1104 (2000)
2. M.U. González, J.M. García, L. González, J.P. Silveira, Y. González, J.D. Gómez, F. Briones, Appl. Suf. Sci. **188**, 188 (2002)
3. H.R. Gutiérrez, M.A. Cotta, M.M.G. de Carvalho, Appl. Phys. Lett. **79**, 3854 (2001)
4. F. Briones, L. González, A. Ruiz, Appl. Phys. A **49**, 729 (1989)
5. P.A. Postigo. Ph.D. thesis., Universidad Politécnica de Madrid, 1996
6. A. Rudra, R. Houdré, J.F. Carlin, M. Ilegems, J. Cryst. Growth **136**, 278 (1994)
7. B. Alén, J. Martínez-Pastor, A. García-Cristobal, L. González, J.M. García, Appl. Phys. Lett. **78**, 4025 (2001)
8. M. Notomi, S. Nojima, M. Okamoto, H. Iwamura, T. Tamamura, Phys. Rev. B **52**, 11073 (1995)
9. E.M. Daly, T.J. Glynn, J.D. Lambkin, L. Considine, S. Walsh, Phys. Rev. B **52**, 4696 (1995)
10. B. Ohnesorge, M. Albrecht, J. Oshinowo, A. Forchel, Y. Arakawa, Phys. Rev. B **54**, 11 532 (1996)
11. M. Gurioli, J. Martínez-Pastor, M. Colocci, C. Deparis, B. Chastaingt, J. Massies, Phy. Rev. B **46**, 6922 (1992)